Available online at www.sciencedirect.com

ScienceDirect

Solid Earth Sciences 4 (2019) 131–141

www.elsevier.com/locate/SESCI

Coral-inferred monsoon and biologically driven fractionation of offshore seawater rare earth elements in Beibu Gulf, northern South China Sea

Xiaohua Li [a,b], Yi Liu [c,d,*], Chung-Che Wu [e], Ruoyu Sun [c,d], Liugen Zheng [f], Mahjoor Ahmad Lone [e], Chuan-Chou Shen [e]

[a] *Center of Deep Sea Research, Institute of Oceanology, Center for Ocean Mega-Science, Chinese Academy of Sciences, Qingdao, 266071, China*
[b] *Laboratory for Marine Mineral Resources, Qingdao National Laboratory for Marine Science and Technology, Qingdao, 266237, China*
[c] *Institute of Surface-Earth System Science, Tianjin University, Tianjin, 300072, China*
[d] *Tianjin Key Laboratory of Earth Critical Zone Science and Sustainable Development in Bohai Rim, Tianjin University, Tianjin, 300072, China*
[e] *High-precision Mass Spectrometry and Environment Change Laboratory (HISPEC), Department of Geosciences, National Taiwan University, Taipei 10617, Taiwan*
[f] *School of Resource and Environment Engineering, Anhui University, Hefei, 230601, China*

Received 13 August 2019; revised 28 September 2019; accepted 28 September 2019
Available online 28 November 2019

Abstract

We present a monthly dataset (AD 2002–2005) of rare earth elements (REEs) recorded in *Porites* coral, which were obtained from the Weizhou Island (WZI), Beibu Gulf, northwest of South China Sea (SCS). This offshore coral shows a strong seasonal cycle in REE/Ca ratios, with enriched REEs (total REEs, 100~140 ppb) in winter and depleted REEs (40~60 ppb) in summer. Since the influence of the river discharge is limited to the river mouth, its contribution to the dissolved REEs is negligible for the offshore area of WZI. Given the similar seasonal pattern of Ba/Ca, we suggest that the remobilization of REEs from river-transported sediments on the shelf of SCS through winter monsoon-driven mixing is the major source of REEs to WZI. Moreover, the peak time of the Nd/Yb ratio (occurred in spring) is not coupled with the occurrence of the maximum REEs, which could mainly be attributed to the degradation of biogenic particles that causes more light REE released in comparison to heavy REE. The Ce anomaly also displays a distinct seasonality (i.e., enhanced anomaly in winter and summer and diminished anomaly in spring), likely reflecting the microbial oxidation activities driven by seasonal temperature and nutrient cycles. Large Gd anomaly (Gd/Gd* up to 1.7) recorded in coral skeletons is unlikely originated from the natural sources, but reflects anthropogenic activities through the recent excessive use of Gd complexes by magnetic resonance imaging of medical examination in this region.

Keywords: Coral; Rare earth element; Winter monsoon; South China sea

1. Introduction

The fourteen rare earth elements (REEs) (La, Ce, Pr, Nd, Sm, Eu, Gd, Tb, Dy, Ho, Er, Tm, Yb and Lu) are a group of a chemically coherent elements. As atomic mass increases, their radii decrease systematically. Distinct REE distribution patterns and abundance anomalies can be identified by normalizing REEs of samples to those of standard shale or chondrite, and have been widely used to anchor the sources and encode geochemical processes (De Baar et al., 1985; McLennan, 1989; Lawrence et al., 2006). REEs are particularly powerful in the studies of aquatic geochemistry (Sholkovitz et al., 1999; Hara et al., 2009; Hatje et al., 2016). Due to the preferential sorption of light REEs (LREEs; La–Eu, larger ionic radius) on the particles and the strong complexation of heavy

* Corresponding author. Institute of Surface-Earth System Science, Tianjin University, Tianjin, 300072, China.
E-mail address: gee@ustc.edu.cn (Y. Liu).
Peer review under responsibility of Guangzhou Institute of Geochemistry.

https://doi.org/10.1016/j.sesci.2019.09.003

REEs (HREEs; Gd–Lu, smaller ionic radius) to solution carbonate, LREEs are depleted in seawater relative to HREEs (De Baar et al., 1985; Byrne and Kim, 1990; Sholkovitz et al., 1994). Cerium is readily oxidized (bacteria involved) to the insoluble tetravalent state and fractionated from other trivalent REEs in seawater, producing a negative Ce anomaly (Elderfield and Greaves, 1982; Elderfield, 1988; Moffett, 1994). The relative abundances of REEs varies regionally across the modern oceans, enabling REEs as robust tracers of continental weathering, oceanic water masses and particle-seawater exchange processes (Zhang and Nozaki, 1998; Sholkovitz et al., 1999; Amakawa et al., 2000). Recently, the large consumption of REE compounds in high-tech products and industrial processes has caused increasing amounts of anthropogenic REEs released into the ocean (Hatje et al., 2016). This has resulted in the enrichment of specific REEs (Gd, La and Sm) in river and coastal waters posing potential ecotoxicological concerns (Bau and Dulski, 1996; Nozaki et al., 2000; Kulaksız and Bau, 2013). However, our knowledge about the seasonal variation and biogeochemical cycles of REEs in the ocean is still limited.

Aragonite skeletons of coral are unique archives recording temporal variations of trace metals in the surface ocean. Trace metals, such as Hg, Cu, Zn, Pb, Mn, Fe, V, Cd, and Ba, in annually banded corals have provided invaluable information on the oceanic processes and recent anthropogenic activities (Shen et al., 1987; McCulloch et al., 2003; Kelly et al., 2009; Saha et al., 2016; Sun et al., 2016; Jiang et al., 2017). REEs could be incorporated into coral aragonite lattice in proportion to seawater concentrations with the distribution coefficients close to one (Sholkovitz and Shen, 1995; Akagi et al., 2004). However, owing to the low concentrations of REEs (total REEs: 1~100 ppb) in coral skeletons, their precise measurement is a great challenge until recent improvement in sample preparation protocols and detection limits of ICP-MS (Akagi et al., 2004; Wyndham et al., 2004; Lewis et al., 2007; Liu et al., 2011; Shen et al., 2011; Saha et al., 2019). High resolution REEs measurement by laser ablation inductively coupled plasma mass spectrometry (LA-ICP-MS) showed that the coastal corals from the Great Barrier Reef (GBR) of Australia were characterized by high REE concentrations and LREE enrichment, indicative of a significant terrestrial influence (Wyndham et al., 2004). Although extremely high REE concentrations (800~2300 ppb) have also been reported in the coastal corals from the Misima Island, Papua New Guinea (Fallon et al., 2002) and Nha Trang Bay, Vietnam (Nguyen et al., 2013), these corals were suspected to be severely impacted by human activities, such as local mining, coastal development, dredging, and dumping. Mostly previous works focused on the use of REEs in coastal corals as a proxy for terrestrial riverine input into coastal areas (Saha et al., 2016, 2019). However, the offshore coral REEs from the shallow reef environments are far less reported (Jiang et al., 2018). Thus, monthly-resolved analysis of coral REEs in different geographic settings is necessary to fully explore the potential of REEs as a tracer of continental and oceanic processes on seasonal scale.

In a previous study by Shen et al. (2011), we developed a method based on an inductively coupled plasma sector field mass spectrometer (ICP-SF-MS), coupled with a microflow nebulizer and a desolvation system, to determine the REEs in corals. This method requires only subpicogram-to-picogram quantities of REEs and 10–20 μg of carbonate. The reported high sensitivity and precision (±1.9–6.5%, 2σ) provided us the opportunity to analyze REEs in the monthly-resolved offshore *Porites* coral from Weizhou Island (WZI) in the Beibu Gulf, northwest of the South China Sea (SCS). Lacking stream inputs and far from rivers, corals from this region receive a minimal quantity of materials brought by continental runoff, and served as an ideal archive of seawater REEs. In this study, we further investigate the seasonal variations of REE pattern and the relevant REE parameters, including Ce anomalies, Gd anomalies, and LREE/HREE ratio, to understand the forcing(s) on seasonal cycling of seawater REEs with limited continental influences. We suggest that offshore coral REEs could provide unique information on the water mixing and stratification, paleogeography, and human activities.

2. Sampling and analytical methods

2.1. Regional settings and coral sample

The Beibu Gulf, covering an area of 126 km^2, is a semi-closed gulf located at the northwest corner of the SCS and southern fringe of East Asia (Fig. 1A). This shallow gulf, with an average depth of <60 m, was formed by the extension of the shelf system of South China. Red River provides the major riverine discharge into the gulf (Liu et al., 2016). Discharge from the Pearl River, 400 km to the northeast, may reach the gulf through the Qiongzhou Strait of 20 km width and 44 m depth (Fig. 1B). The gulf has a typical subtropical climate situated in the East Asian monsoon realm. During May to September, the southwest summer monsoon and occasional typhoons bring the seasonal rainfall of ~1400 mm, more than 88% of the yearly precipitation (2002–2005) (Fig. S1). From October to March, the prevailing northeast winter monsoon brings cold and dry continental air masses from Siberian high. The average sea surface temperature (SST) during 2002–2005 ranges from 19.1 °C in winter to 30.3 °C in summer (Fig. 2D).

A core WZI-09-2-1, 20 cm in length and 5 cm in diameter, was drilled from the top of a living *Porites lutea* coral at a water depth of 7 m near WZI in the year 2009. WZI, a small volcanic island with an area of 24.7 km^2, is mainly composed of alkaline basalt, including alkaline olivine basalt and picrite (Fan et al., 2008). This primitive island, isolated from Asian continent, is an offshore area at the northeast of the Beibu Gulf and the northern limit of coral reef distribution belt of the SCS (Yu et al., 2004). Recently, WZI reefs are disturbed by increasing human activities, such as oil spill events, constructions of offshore oil platforms (Xu et al., 2018).

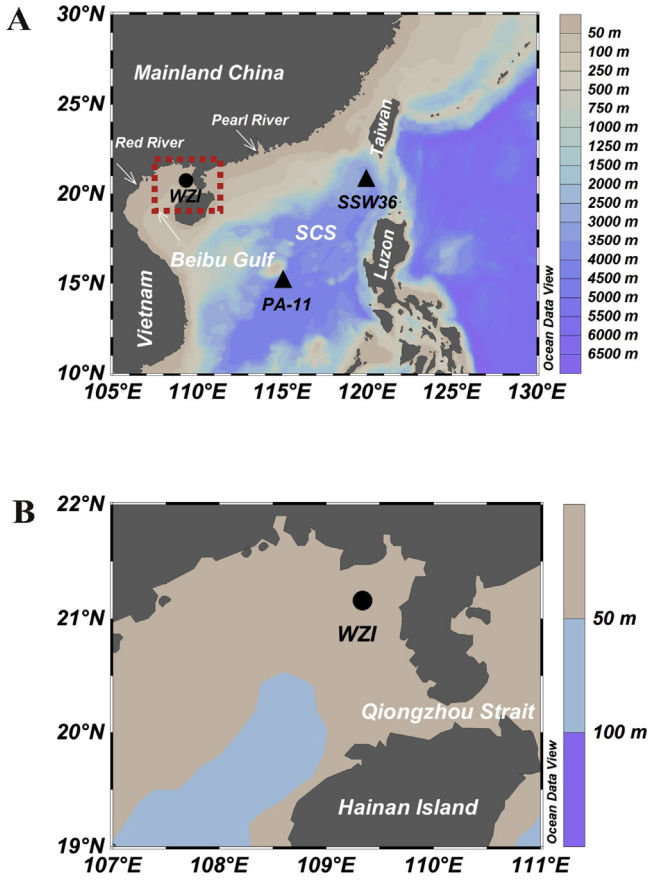

Fig. 1. Bathymetric map of the South China Sea (SCS) showing the locations of (A) Beibu Gulf and (B) Weizhou Island (WZI). The circle indicates the sample site of WZI coral used in this study, and triangles indicate the open surface seawater of the SCS (station PA-11) and surface seawater near Luzon Strait (station SSW 36) which were measured by Amakawa et al. (2000) for REEs. The map was created using ODV (Schlitzer, 2015).

2.2. Analytical methods

2.2.1. Subsampling process and chemical treatment

A 5-mm-thick slice was cut from coral core WZI-09-2-1, washed with deionized water, and dried for X-ray photographing (Fig. S2). Based on the annual density bandings on X-ray photographs, the growth rate of this coral is estimated to be 7–8 mm/year.

Subsample cubes ($1 \times 1 \times 1$ mm^3), 7–8 per year, spanning from 2002 to 2005, were cut along the maximum growth axis of the coral slice using the micro-surgical subsampling technique (Shen et al., 1996). After crushing into powder, the subsamples were cleaned with 10% H_2O_2 and ultrapure water in an ultrasonic bath. The cleaned subsamples were dissolved using 5% HNO_3 in Teflon vials before analysis. Matrix-matched standard was prepared by dissolving super-pure calcium (purity $\geq$ 99.999%, Sigma–Aldrich Inc.) and REE multi-element standard solution (10 μg/ml with an accuracy of ±0.5%, high-purity) in 3% HNO_3 (Shen et al., 2011). All chemical procedures were performed on a class-100 laminar-flow bench in a class-10,000 clean room in the High-precision Mass Spectrometry and Environment Change Laboratory (HISPEC), the Department of Geosciences, National Taiwan University (Shen et al., 2006).

2.2.2. Instrumental analyses

The dissolved subsample solution with ~400 ppm of Ca was divided into two aliquots. One was diluted with 40-ppm Ca for REE/Ca measurements (Shen et al., 2011). A standard-bracketing method was used for elemental ratio determination on a single secondary electron multiplier of an ICP-SF-MS, Element II (Thermo Electron, Bremen, Germany), under a hot-plasma condition with RF power of 1200 W. A desolvation nebulization device, Aridus (CETAC Technologies, NE), was used as the introduction system to minimize spectral interference and the formation of hydrides and oxides of REEs and to enhance instrumental sensitivity (Shen et al., 2011). Ion beams including ^{46}Ca, ^{139}La, ^{140}Ce, ^{141}Pr, ^{146}Nd, ^{147}Sm, ^{153}Eu, ^{160}Gd, ^{159}Tb, ^{163}Dy, ^{165}Ho, ^{166}Er, ^{169}Tm, ^{172}Yb and ^{175}Lu were detected. Every four samples were bracketed with one matrix-matched standard. All REE/Ca ratios were calculated directly from ratios of ion beam intensities after correcting for blanks, instrumental mass discrimination and ratio drifting using the external matrix-matched standards. The two-month 2-sigma reproducibility is ±1.9–6.5% for REE/Ca ratios. The detailed instrumental settings and analytical details are described in Shen et al. (2011). The total REE concentrations were calculated from the determined REE/Ca ratios and the Ca concentration of 9.52 mmol/g for *Porites* corals in the SCS (Sun et al., 2005).

Another aliquot was diluted with 3-ppm Ca for Sr/Ca and Ba/Ca analyses by a standard-bracketing method on the same SF-ICP-MS (Lo et al., 2014). A cold-plasma condition with RF power of 800 W was set. A quartz Scott-type double-pass spray chamber was employed for sample introduction. Ion beams of ^{43}Ca, ^{86}Sr and ^{138}Ba were measured at a low resolution ($M/\Delta M = 300$) and peak hopping mode (Lo et al., 2014). The six-month 2-sigma reproducibility is ±0.4% for Sr/Ca and ±0.2% for Ba/Ca.

Coralline aragonite Sr/Ca is considered as a robust SST proxy (Shen et al., 1996). Coral trace elemental records are thus calendared by matching Sr/Ca maxima (Fig. 2C) to the instrumental SST minima and an assumed constant intra-annual growth rate (Fig. 2D).

3. Results

3.1. Temporal variations of REE/Ca and Ba/Ca

Measured REE/Ca ratios for the WZI coral are listed in Table 1. The individual REE/Ca ratios vary from 2 to 20 nmol/mol for LREEs (La–Eu), and from 0.3 to 5 nnol/mol for HREEs (Gd–Lu). Variations of total REEs, Ba/Ca, and Sr/Ca along the growth axis of the studied coral during 2002–2005 are illustrated in Fig. 2A–C. Notably, the total REEs display a strong seasonal cyclicity with high values of 100–140 ppb in winter and low values of 40–60 ppb in summer (Fig. 2A).

All the individual REE time series show large variations and mutually significant correlations (Table 2). The correlation

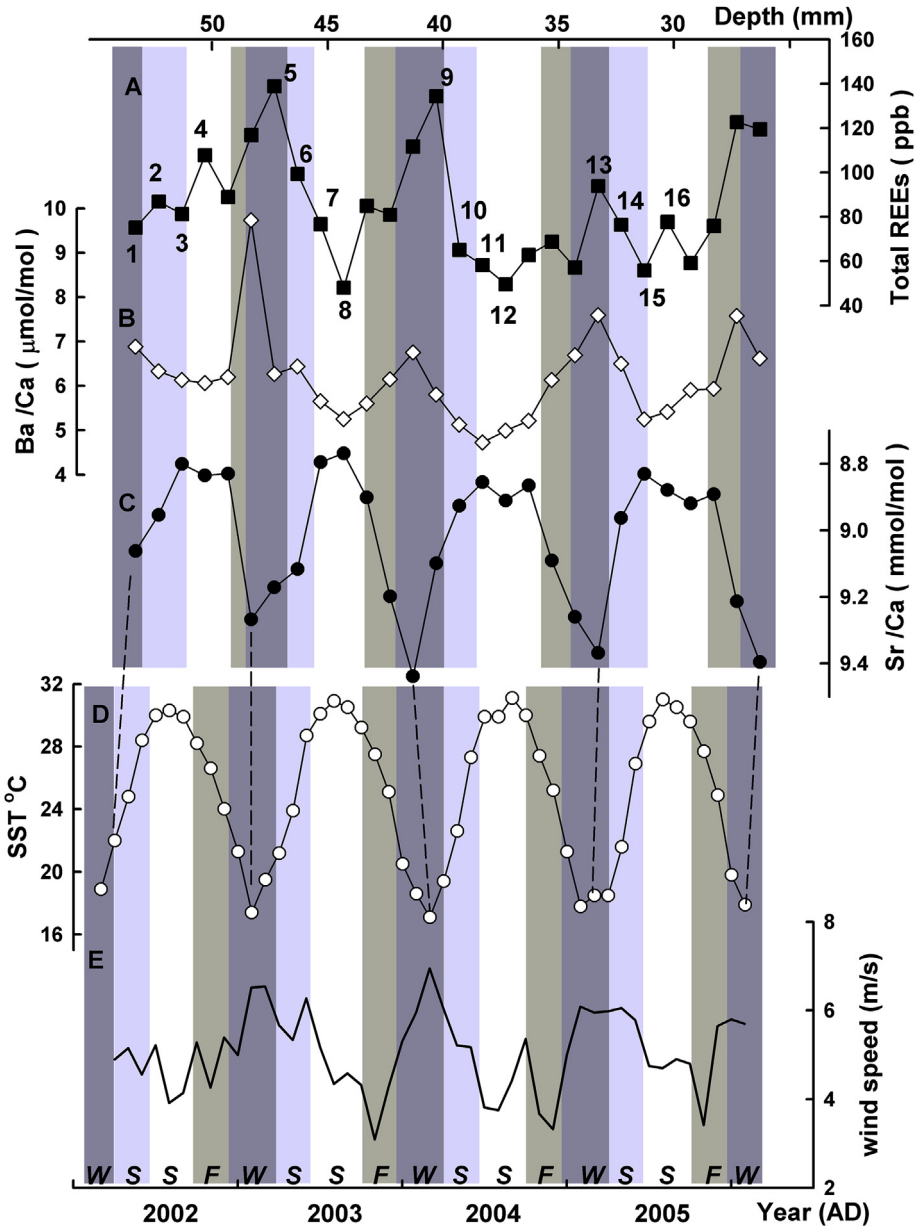

Fig. 2. Seasonal variations of (A) total REEs; (B) Ba/Ca; (C) Sr/Ca; (D) SST and (E) wind speed of WZI. The REE/Ca and Ba/Ca along the coral growth axis was transformed into a time series by matching Sr/Ca to instrumental SST data (see details in section 3.1). SST data is from WZI meteorological station. Wind speed is from https://www.esrl.noaa.gov/. The REE patterns of the numbered sample points (1−16) in Fig. 2A are shown in Fig. 6.

coefficients (R) are as high as 0.91−0.99 between neighboring REEs and 0.7−0.9 among LREEs and HREEs. Ce shows the weakest correlation with neighboring REEs (0.9) and HREEs (0.7).

3.2. Normalized REEs ratios

The PAAS-normalized (McLennan, 1989) REE distribution pattern of WZI coral during 2002−2005 is depicted in Fig. 3, along with those of Chinese loess (Liu et al., 1993), red earth in South China (Xiong et al., 2002), WZI volcanic rocks (Fan et al., 2008), unfiltered winter surface seawater of WZI (Ge et al., 2008), open surface seawater of SCS and surface seawater near Luzon Strait (Amakawa et al., 2000). The REE pattern in WZI coral is characterized with a negative Ce anomaly, a positive Gd anomaly, and an enrichment of HREEs over LREEs. Such attributes are consistent with typical REE features of shallow, oxic seawater, corroborating the previous studies that coral REE patterns can reliably mirror those of ambient seawater (Sholkovitz and Shen, 1995; Akagi et al., 2004; Wyndham et al., 2004; Saha et al., 2019).

Gd and Ce anomalies are calculated by geometrically extrapolating Tb and Dy, Pr and Nd respectively (Lawrence et al., 2006) and is given as follows:

Table 1
Summary of REE/Ca ratio (nmol/mol), Ce and Gd anomalies, and Nd/Yb ratio (mol/mol) in WZI coral.

Sample No.	La	Ce	Pr	Nd	Sm	Eu	Gd	Tb	Dy	Ho	Er	Tm	Yb	Lu	Ce/Ce*	Gd/Gd*	Nd/Yb
WZI-1	12.8	6.87	2.38	10.3	2.29	0.64	3.26	0.60	4.19	1.05	3.35	0.47	3.01	0.46	0.37	1.05	3.43
WZI-2	14.7	9.01	2.85	12.5	2.76	0.71	4.19	0.62	4.73	1.11	3.26	0.43	2.72	0.44	0.41	1.41	4.61
WZI-3	14.1	8.35	2.79	12.3	2.60	0.66	4.06	0.60	4.02	0.96	2.93	0.39	2.23	0.31	0.39	1.24	5.52
WZI-4	17.7	9.95	3.52	15.7	3.61	0.83	5.56	0.79	5.93	1.42	4.43	0.55	3.67	0.60	0.37	1.46	4.26
WZI-5	15.1	8.93	2.96	13.2	2.72	0.74	3.64	0.67	4.55	1.18	3.72	0.49	2.97	0.45	0.40	1.04	4.46
WZI-6	19.9	10.3	3.79	16.3	3.9	0.89	6.18	0.87	6.17	1.53	4.81	0.66	4.43	0.71	0.34	1.40	3.69
WZI-7	24.1	13.0	4.63	20.5	4.23	1.12	6.69	0.95	7.23	1.75	5.39	0.73	4.81	0.74	0.37	1.50	4.26
WZI-8	17.9	12.0	3.49	14.7	3.24	0.86	4.53	0.65	4.58	1.06	3.09	0.39	2.42	0.38	0.42	1.38	6.06
WZI-9	13.8	8.29	2.73	11.9	2.50	0.58	3.24	0.48	3.36	0.84	2.58	0.35	2.29	0.35	0.39	1.29	5.19
WZI-10	7.87	4.01	1.51	6.84	1.50	0.35	2.78	0.35	2.79	0.70	2.08	0.29	1.70	0.26	0.35	1.75	4.03
WZI-11	13.9	7.65	2.62	12.0	2.78	0.67	4.31	0.63	4.68	1.13	3.76	0.52	3.13	0.54	0.39	1.42	3.83
WZI-12	13.3	6.84	2.60	10.9	2.58	0.67	3.92	0.60	4.74	1.14	3.69	0.52	3.47	0.51	0.32	1.43	3.13
WZI-13	18.3	9.30	3.55	15.4	3.59	0.92	5.63	0.88	6.28	1.53	5.07	0.74	4.72	0.72	0.33	1.28	3.26
WZI-14	22.2	11.5	4.25	19.1	4.64	1.19	6.96	1.00	7.27	1.76	5.59	0.78	5.20	0.88	0.36	1.41	3.66
WZI-15	11.2	6.77	2.18	9.91	2.19	0.51	3.20	0.45	3.04	0.79	2.32	0.32	1.89	0.29	0.41	1.31	5.26
WZI-16	9.94	5.53	1.91	8.51	1.78	0.51	2.87	0.47	3.10	0.79	2.35	0.31	1.83	0.28	0.38	1.11	4.66
WZI-17	8.20	4.20	1.63	6.84	1.40	0.36	2.33	0.40	2.85	0.73	2.35	0.34	2.01	0.33	0.32	1.14	3.41
WZI-18	9.92	5.48	1.93	8.37	1.87	0.52	3.41	0.50	3.68	0.87	2.97	0.37	2.62	0.44	0.36	1.41	3.19
WZI-19	10.8	5.52	2.17	9.98	2.05	0.6	3.59	0.53	3.95	0.99	3.10	0.43	2.90	0.45	0.35	1.41	3.45
WZI-20	9.12	4.95	1.81	7.72	1.66	0.48	2.96	0.40	3.17	0.86	2.72	0.38	2.48	0.40	0.34	1.66	3.12
WZI-21	15.8	8.64	3.09	13.1	2.76	0.76	4.42	0.69	4.94	1.28	4.09	0.56	3.85	0.57	0.35	1.28	3.41
WZI-22	13.2	7.62	2.66	11.1	2.26	0.6	3.66	0.60	3.90	0.95	3.05	0.38	2.44	0.36	0.35	1.11	4.56
WZI-23	9.33	5.68	1.77	7.51	1.61	0.42	2.52	0.36	3.09	0.75	2.44	0.36	2.24	0.35	0.40	1.70	3.35
WZI-24	16.1	8.77	2.16	9.32	2.05	0.53	3.04	0.52	3.81	0.89	2.97	0.41	2.79	0.44	0.52	1.18	3.34
WZI-25	11.5	6.14	1.74	7.81	1.57	0.45	2.34	0.47	3.01	0.77	2.45	0.32	2.03	0.29	0.46	0.88	3.84
WZI-26	12.0	8.6	2.29	9.55	2.33	0.5	4.25	0.56	4.46	0.93	2.99	0.45	2.81	0.46	0.46	1.68	3.40
WZI-27	20.0	11.3	3.55	15.6	3.96	0.96	6.46	0.96	6.97	1.71	5.54	0.80	5.33	0.92	0.41	1.37	2.93
WZI-28	18.7	9.70	3.56	15.4	3.70	1.08	6.84	0.96	7.44	1.69	5.50	0.77	5.33	0.90	0.34	1.54	2.88

Table 2
Correlation coefficient (R) matrix between individual REEs in WZI coral.

	Ce	Pr	Nd	Sm	Eu	Gd	Tb	Dy	Ho	Er	Tm	Yb	Lu
La	0.955	0.967	0.964	0.955	0.943	0.902	0.934	0.912	0.913	0.887	0.853	0.842	0.814
Ce		0.932	0.922	0.907	0.875	0.835	0.850	0.828	0.808	0.769	0.732	0.714	0.693
Pr			0.996	0.977	0.964	0.927	0.937	0.917	0.922	0.887	0.845	0.829	0.797
Nd				0.979	0.965	0.926	0.937	0.915	0.924	0.888	0.844	0.825	0.796
Sm					0.969	0.966	0.963	0.952	0.952	0.926	0.898	0.880	0.867
Eu						0.949	0.968	0.957	0.961	0.938	0.904	0.895	0.876
Gd							0.967	0.980	0.966	0.951	0.931	0.924	0.922
Tb								0.982	0.983	0.974	0.949	0.939	0.923
Dy									0.990	0.984	0.968	0.964	0.954
Ho										0.993	0.975	0.969	0.954
Er											0.989	0.986	0.973
Tm												0.992	0.982
Yb													0.990

$$\frac{Gd}{Gd^*}=\frac{(Gd/Gd_{shale})\times(Dy/Dy_{shale})}{(Tb/Tb_{shale})\times(Tb/Tb_{shale})} \quad (1)$$

$$\frac{Ce}{Ce^*}=\frac{(Ce/Ce_{shale})\times(Nd/Nd_{shale})}{(\mathrm{Pr}/\mathrm{Pr}_{shale})\times(\mathrm{Pr}/\mathrm{Pr}_{shale})} \quad (2)$$

Gd/Gd* in WZI coral varies significantly, from 0.88 to 1.75 (Fig. 4A). Four samples (WZI-10, 20, 23 and 26 in Table 1) exhibited extremely high Gd anomalies (~1.7) where the total REE concentrations were low (<80 ppb). After excluding these four samples, a significant positive correlation between total REEs and Gd anomaly ($R = 0.58$, $p = 0.03$, Fig. 4B) is observed.

Ce/Ce* in WZI coral varies from 0.3 to 0.5 (Fig. 5B and Table 1), which is within the range of Ce anomalies observed in seawater (Wyndham et al., 2004). The negative Ce anomaly is a well-established feature in oxic seawater, because the oxidation of Ce(III) to Ce(IV) results in a preferential removal of insoluble Ce(IV) from seawater (Moffett, 1994). Like total REEs, Ce/Ce* reveals a strong seasonal cycle (Fig. 5B). However, no significant correlation is observed between total REEs and Ce/Ce* ($R = 0.12$, $p = 0.55$).

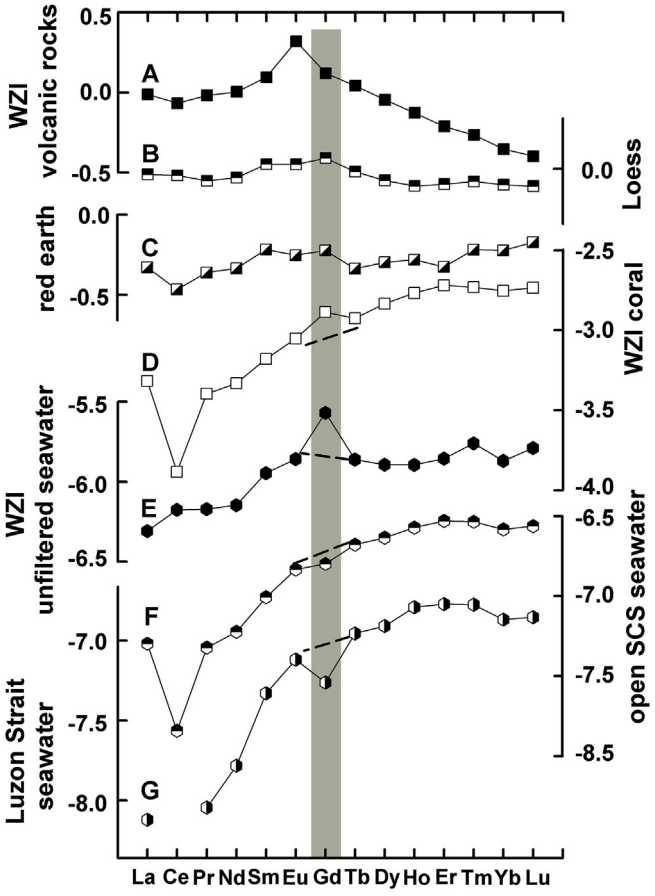

Fig. 3. PAAS-normalized REE patterns of (A) WZI volcanic rocks (Fan et al., 2008), (B) Chinese loess (Liu et al., 1993), (C) red earth in south China (Xiong et al., 2002), (D) WZI coral (this study), (E) unfiltered surface seawater of WZI (Ge et al., 2008), (F) open surface seawater of the SCS (station PA-11) and (G) surface seawater near Luzon Strait (station SSW 36) (Amakawa et al., 2000). REE pattern for the WZI coral represents the average values of the analyzed sections.

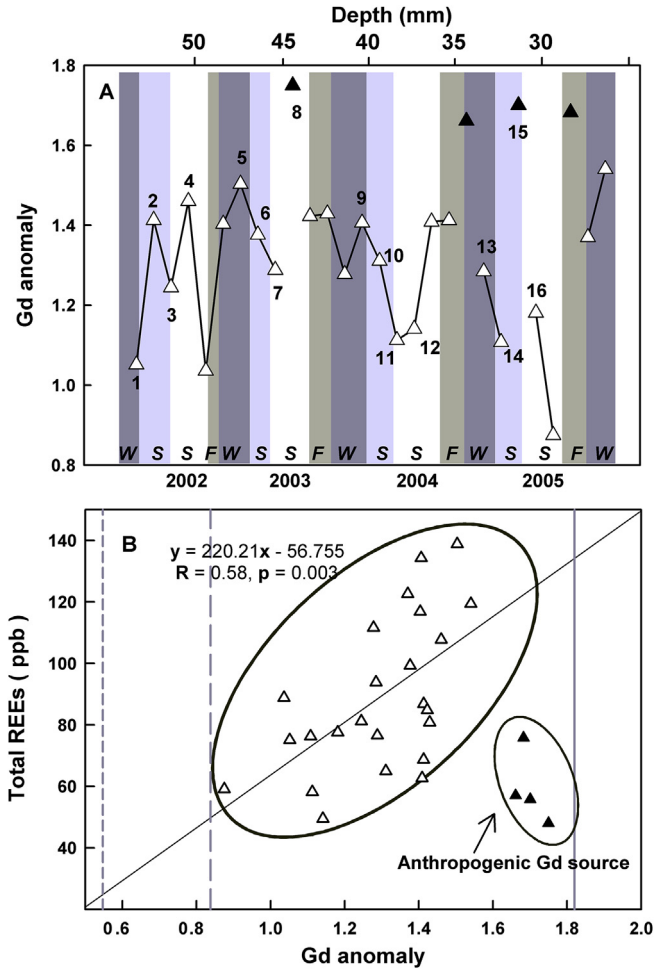

Fig. 4. Seasonal cycle of Gd anomaly in (A) WZI coral and (B) the relationship between Gd anomaly and total REEs concentrations. Samples in the ellipse in Fig. 4B reveal abnormally high Gd anomaly and their corresponding points (solid triangles) are indicated in Fig. 4A. The vertical lines in Fig. 4B, from left to right, denote the values of Gd anomaly in unfiltered surface seawater of WZI (Ge et al., 2008), open surface seawater of the SCS (station PA-11) and surface seawater near Luzon Strait (station SSW 36) (Amakawa et al., 2000), respectively.

Nd/Yb ratio is one way to describe the enrichment or depletion of LREEs relative to HREEs (Wyndham et al., 2004), and it's ratios in WZI coral are plotted in Fig. 5A. Also displaying seasonal cyclicity, Nd/Yb peaks around 5–6 in spring and stabilizes around 3–4 in other seasons. Furthermore, a considerable positive correlation with Ce anomaly ($R = 0.61$, $p = 0.0011$, Fig. 5C) is observed, however, no significant correlation is exhibited between Nd/Yb and total REEs ($R = 0.05$, $p = 0.81$).

4. Discussions

4.1. Sources of the coral REEs

To decode the source of REEs incorporated into the studied coral, we delved into following possible sources: (a) discharge of rivers from the Asian continent, (b) local erosion within WZI, (c) distant eolian input, and (d) remobilization of sediments on the shelf.

Riverine source of REEs cannot explain the temporal patterns of coral REEs. As shown in Fig. S1, more than 88% of the yearly precipitation in this region occurs between May to September. Heavy rainfall usually brings large amounts of terrestrial REEs into coastal seawater (Fallon et al., 2002; Wyndham et al., 2004). However, our coral REEs exhibit highest values during winter (December to February) associated with very limited precipitation. Furthermore, the studied coral site is far from river sources. Therefore, the riverine source of REEs in WZI seems negligible, especially during winter season marked with declined terrestrial flux. This is consistent with the observations by Amakawa et al. (2000) who showed that the input of river-dissolved REEs to the offshore regions of SCS is negligible.

Weathering and erosion of volcanic rocks is suggested as an important seawater REEs source, as indicated in the case studies from Philippine and Indonesian Archipelago

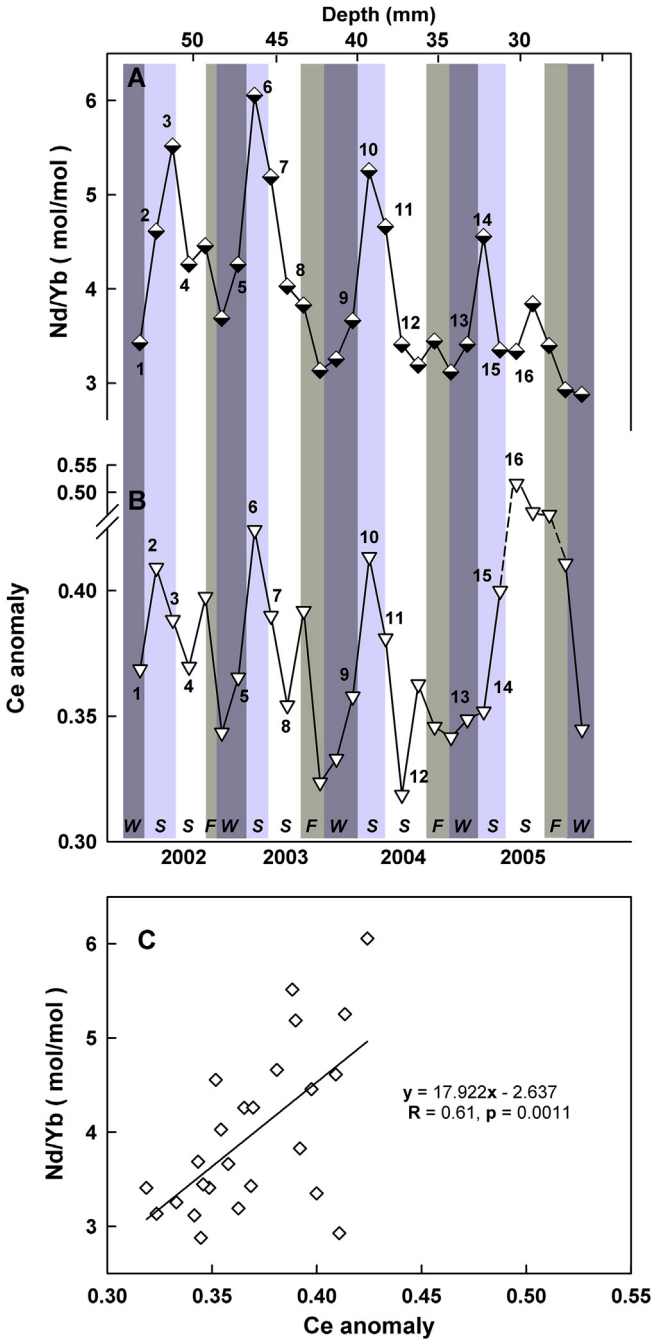

Fig. 5. Seasonal cycle of (A) Nd/Yb ratios, (B) Ce anomaly in WZI coral and (C) the relationship between Nd/Yb and Ce anomaly.

(Sholkovitz et al., 1999). However, the erosion and transport of terrestrial materials in tropical islands occur mostly during wet summer monsoon (Liu et al., 2015), excluding the likelihood of local erosion as a source of REEs within WZI. Furthermore, the PAAS-normalized REEs pattern of volcanic rocks in WZI is characterized by an enrichment of LREEs and a strong Eu enrichment (Fig. 3A) (Fan et al., 2008), which is quite different from what is observed in the studied coral (Fig. 3D).

Eolian dust followed by the solubilization of particle-bound REEs in the seawater has been suggested to be an important source for the REEs in the western North Pacific Ocean (Greaves et al., 1999), but this conclusion was later retracted (Greaves et al., 2001). And a previous study shows that the REE concentration in the offshore seawaters of SCS is enriched by a factor of >2 compared to the western North Pacific Ocean which is under direct transport path of Asian eolian dust (Amakawa et al., 2000). Moreover, the surface seawater in SCS is reported with very low values of ^{210}Pb, a tracer for atmospheric deposition (Nozaki et al., 1998). Besides, the shale-normalized flat REE pattern of eolian dust is distinctively different from the coral pattern (Fig. 3). The shift from a Ce-depleted pattern to a flat pattern in surface seawater probably reflects the input of wind-blown Asian dust in the Xisha (Jiang et al., 2018), which is not observed in our study. Thus, the contribution of eolian dust to REEs at least in offshore WZI is small.

We suggest that the dissolution of particulate REE phases within shelf sediments, followed by the winter monsoon driven mixing sources REEs to offshore seawater in WZI. Although the direct input of river-dissolved REEs to the offshore seawater is quite limited, a large amount of river-transported sediments are accumulated on the shelf area of SCS (Liu et al., 2016). The continental shelf areas of the SCS are as large as 1.8 million km^2 (Wang et al., 1997), and receive ~700 million metric tons (Mt)/year of river-transported sediments from the surrounding large rivers such as Pearl River (84 Mt/year), Red River (130 Mt/year) and Mekong River (160 Mt/year) (Liu et al., 2016). Shelf sediments are an important source of dissolved trace metals in the ocean (Spivack and Wasserburg, 1988). The concentration of dissolved REEs in sediment pore water is much higher than that of seawater (Haley et al., 2004). Upwelling and lowering of SST induced by strong winter monsoon (Fig. 2D and E) could effectively weaken the seawater stratification, thereby, developing a well-mixed seawater during winters across the shallow Beibu Gulf (Tang et al., 2003). A coupled effect of remobilization and mixing thus leads the dissolved REEs in the bottom sediments to surface, contributing positively to the REE budget of the offshore sea water in the Gulf. Interestingly, we observed higher REE values in the studied coral during winter seasons, coincident with the prevailing northeast monsoon with higher wind speed (Fig. 2). In contrast, the observed low REE concentrations during summer are possibly related to seawater stratification caused by increased SST and lower wind speed. Our proposed mechanism is further supported by the synchronous seasonal changes between Ba/Ca (Fig. 2B) and total REEs ($R = 0.55$, $p = 0.0025$). Pore-water Ba concentrations are also higher than that of seawater (Paytan and Kastner, 1996). Furthermore, our coral record shows a distinctly positive Gd anomaly ($Gd/Gd^* = 1.4 \pm 0.42$, 2σ, Fig. 3D) which significantly correlates with total REEs ($R = 0.58$, $p = 0.03$, excluding samples WZI-10, 20, 23 and 26). Positive Gd anomaly has been reported in the weathered soils and rocks (Braun et al., 1990; Koppi et al., 1996; Ma et al., 2007), and in corals from central Vietnam shelf, western SCS ($Gd/Gd^* = 1.3–1.4$) (Nguyen et al., 2013). In contrast, the open seawater of SCS is influenced by the western North Pacific

seawater (Gd/Gd* = 0.55, Fig. 3G) (Alibo and Nozaki, 2000) through Taiwan and Luzon Strait (Fig. 1) and is reported with a slightly negative Gd anomaly (Gd/Gd* = 0.88, Fig. 3F) (Amakawa et al., 2000). Therefore, the positive Gd anomaly and its significant correlation with REEs in the studied coral further indicate the remobilized REEs from the shelf sediments as a primary contributor to the dissolved REE budge of WZI offshore seawater.

Conspicuously, four coral subsamples (WZI-10, 20, 23 and 26, given in Table 1) show extremely high Gd anomaly values (Gd/Gd*, ~1.7). These anomalous values are observed where the total REE concentrations are low (<80 ppb) (Fig. 4B). Unfiltered seawater of WZI collected in 2007 also exhibited an extremely high Gd anomaly (Gd/Gd* = 1.8; Ge et al., 2008) (Fig. 3E). It is unlikely that these large anomalous Gd values are derived from the natural sources or the fractionation of REEs. Recently, extremely positive Gd anomaly (Gd/Gd* = 1.6–3) has been reported in the contaminated seawater of San Francisco Bay and Tokyo Bay, presumably related to the widespread use of Gd complexes in magnetic resonance imaging (MRI) for medical examination (Nozaki et al., 2000; Kulaksız and Bau, 2013; Hatje et al., 2016). South China is one of the most populous and fastest growing regions in the world. Large scale human activity is anticipated to source excess anthropogenic Gd (Hatje et al., 2016) resulting in its significant enrichment in the gulf. To our knowledge, this is the first report of anthropogenic Gd contamination recorded in a natural archive in SCS. Therefore, the REE anomalies recorded in corals could potentially serve as a new tracer of anthropogenic REEs in the seawater through Anthropocene.

4.2. LREEs and HREEs fractionation

Nd/Yb time series from our coral record reveal a clear fractionation between LREEs and HREEs during spring compared to other three seasons (Fig. 5A). To investigate the mechanisms for this fractionation of Nd/Yb, detailed REE patterns of WZI coral from winter to summer are illustrated for each year in Fig. 6.

Generally, offshore seawater is characterized by enriched HREEs (low Nd/Yb ratio), while as coastal waters are relatively augmented in LREEs (high Nd/Yb ratio) due to terrestrial flux (Saha et al., 2016, 2019). As reported in Okinawa Island, both Nd/Yb ratios and REE concentrations were higher in seawater and corals that received terrestrial runoff than those distant from riverine sources (Akagi et al., 2004). Similarly, coastal corals of GBR subjected to terrestrial influence were more enriched in REEs and revealed higher Nd/Yb ratios than the mid-shelf corals (Wyndham et al., 2004). These researchers found high Nd/Yb ratios consistent with summer flooding events from the nearby Burdekin River (Wyndham et al., 2004). However, our studied coral reveals Nd/Yb peaks in spring (4.6–6.1, Fig. 5A) and exhibits no correlation with total REEs ($R = -0.05$, $p = 0.81$) which are otherwise high during winter (Fig. 2A). This further confirms that the coral REEs were not derived directly from the terrestrial sources. We suggest that the seasonal cycle in coral Nd/Yb is caused by mineralization and desorption processes occurring on the biogenic particles in seawater.

During winter, the strong northeast monsoon not only brings REEs to the surface, but also nutrients, supporting phytoplankton bloom (Tang et al., 2003). Following this phytoplankton bloom, a large amount of biogenic particles are generated (Ma et al., 2014). The satellite images in Figs. S3-S4 shows elevated levels of Chlorophyll-a (Chl-a) and particulate organic carbon (POC) concentrations during winter in the Beibu Gulf. As the northeast monsoon retreats, Chl-a and POC concentrations decrease sharply following the onset of spring (Figs. S3-S4). The net mineralization of biogenic particles in spring would release more LREEs than HREEs (Hara et al., 2009), thus producing coral Nd/Yb peaks during spring (Fig. 5A). The REE patterns ([2], [3], [6], [7], [10], [11] and [14] in Fig. 6) in each spring did show that the increase in Nd/Yb is largely as a result of LREE release (La–Eu). With the end of spring or beginning of summer, this process finishes and the REE pattern returns to ones similar to other seasons (Fig. 6).

4.3. Seasonal cycle of Ce anomaly

Our coral displays the most negative (enhanced) Ce anomaly during summer and winter, indicating intense oxidization of Ce (III) in seawater during these seasons. Summer associated enhancement of Ce anomaly in seawater was first reported in Chesapeake Bay by Moffett (1994), who observed a significantly lower Ce anomaly in winter (~0.18) than summer (0.35–0.45). GBR coastal corals near the mouth of Burdekin River in Australia also showed a similar enhanced negative Ce anomaly during summer (Wyndham et al., 2004). It has been suggested that the changes in Ce anomaly are primarily controlled by the abundance of Ce oxidizing bacteria, which increases during summer due to high temperature and/or strong solar radiation. Moffett (1994) indicated that the specific Ce oxidation rate during summer increased by 200 times compared to winter. Surprisingly, apart from summer, the enhanced Ce anomaly is also observed during winter in our sample which is contrary to previous observations by other workers (Wyndham et al., 2004). This is likely related to enhanced Ce oxidation by high levels of nutrient brought up by winter monsoon. Furthermore, a low Ce anomaly is observed during spring, which could be linked to the transient reducing conditions induced by the degradation of biogenic particles in such a high productive region. This is consistent with the process, we proposed for Nd/Yb peaks for the same season. Under reducing condition, Ce(IV) is reduced to Ce(III) and released back to the seawater (Haley et al., 2004).

It is noted that the Ce anomaly is relatively higher during summer of 2005 (0.46–0.52) (Sample WZI-24, 25 and 26 in Table 1). Instrumental record shows that summer SST during 2005 was as high as 31 °C (typically ~30 °C) but the rainfall was only ~1100 mm (typically ~1400 mm). We suspect that the combined effects of thermal and saline stress might disrupt the coral metabolism and the associated Ce incorporation.

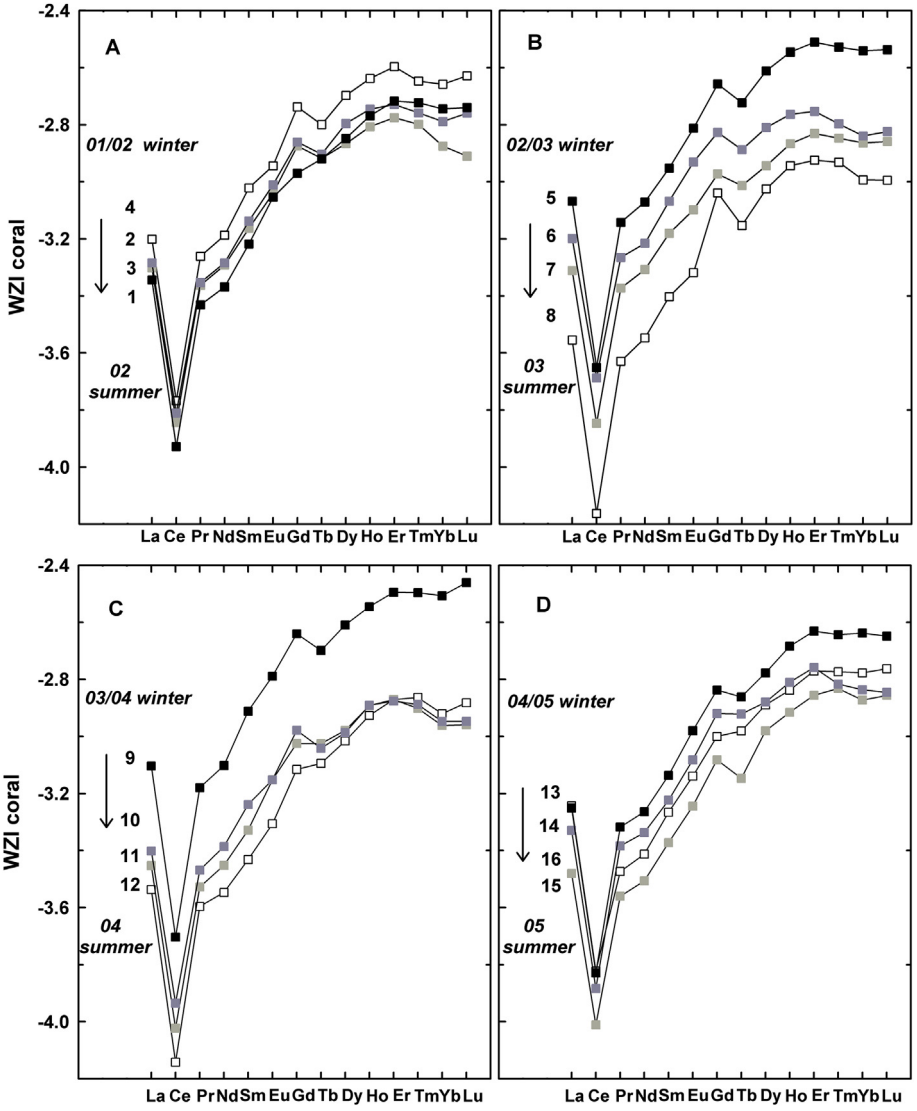

Fig. 6. The variations of REE pattern in WZI coral from late winter to early summer during 2002–2005. The numbered points beside each REE pattern corresponds to those in Fig. 2A.

5. Conclusions

Monthly-resolved record of REEs in an offshore coral from WZI, Beibu Gulf, SCS is presented with high precision analytical protocols. We found that the remobilization and mixing during winter monsoon plays a key role in REE seasonality in offshore seawater. Remobilization of REEs from river-transported sediments on the shelf of SCS is identified as an important source of dissolved REEs. The coral record of Nd/Yb shows a strong seasonal cycle, exhibiting highest values during spring and appears to be primarily controlled by LREE release processes following the degradation of biogenic particles. Ce anomaly also displays a strong seasonal cycle, with enhanced anomalies during summer and winter. The former is likely caused by increased Ce oxidation rates due to enhanced solar radiation and summer SST, while the latter appears to be related to high productivity. Extremely high Gd anomaly (Gd/Gd* = ~1.7) recorded in the coral indicates increased input of the anthropogenic Gd in recent years. The seasonal patterns of various REE parameters highlight the potential of corals as a recorder of historical REEs cycling in marine environments.

Conflict of interests

The authors declare that they have no known competing financial interests or personal relationships that could have appeared to influence the work reported in this paper.

Acknowledgements

This research was supported by the National Key Basic Research Program of China (2013CB956102), the National Science Foundation of China (41922019, 441572148), the Open foundation of State Key Laboratory of Loess and Quaternary Geology (SKLLQG1613), and China Postdoctoral

Science Foundation Grant (2019M652490). Grants from Taiwan MOST (105-2119-M-002-001, 106-2628-M-002-013 to C.-C.S.) and the National Taiwan University (105R7625 to C.-C.S.) are also thanked. We are grateful to Xing Wang and Guang-Zhao Li for their assistance during the sample collection.

Appendix A. Supplementary data

Supplementary data to this article can be found online at https://doi.org/10.1016/j.sesci.2019.09.003.

References

Akagi, T., Hashimoto, Y., Fu, F.F., Tsuno, H., Tao, H., Nakano, Y., 2004. Variation of the distribution coefficients of rare earth elements in modern coral-lattices: species and site dependencies. Geochem. Cosmochim. Acta 68 (10), 2265−2273. https://doi.org/10.1016/j.gca.2003.12.014.

Alibo, D.S., Nozaki, Y., 2000. Dissolved rare earth elements in the South China Sea: geochemical characterization of the water masses. J. Geophys. Res. 105 (C12), 28771−28783. https://doi.org/10.1029/1999JC000283.

Amakawa, H., Alibo, D.S., Nozaki, Y., 2000. Nd isotopic composition and REE pattern in the surface waters of the eastern Indian Ocean and its adjacent seas. Geochem. Cosmochim. Acta 64 (10), 1715−1727. https://doi.org/10.1016/S0016-7037(00)00333-1.

Bau, M., Dulski, P., 1996. Anthropogenic origin of positive gadolinium anomalies in river waters. Earth Planet. Sci. Lett. 143 (1−4), 245−255. https://doi.org/10.1016/0012-821X(96)00127-6.

Byrne, R.H., Kim, K.H., 1990. Rare earth element scavenging in seawater. Geochem. Cosmochim. Acta 54 (10), 2645−2656. https://doi.org/10.1016/0016-7037(90)90002-3.

Braun, J.J., Pagel, M., Muller, J.P., Michard, A., Guillet, B., 1990. Cerium anomalies in lateritic profiles. Geochem. Cosmochim. Acta 54 (3), 781−795. https://doi.org/10.1016/0016-7037(90)90373-S.

De Baar, H.J.W., Brewer, P.G., Bacon, M.P., 1985. Anomalies in rare-earth distributions in seawater - Gd and Tb. Geochem. Cosmochim. Acta 49 (9), 1961−1969. https://doi.org/10.1016/0016-7037(85)90090-0.

Elderfield, H., Greaves, M.J., 1982. The rare earth elements in seawater. Nature 296 (5854), 214−219. https://doi.org/10.1038/296214a0.

Elderfield, H., 1988. The oceanic chemistry of the rare-earth elements. Philos. Trans. R. Soc. London, Ser. A 325 (1583), 105−126. https://doi.org/10.1098/rsta.1988.0046.

Fallon, S.J., White, J.C., McCulloch, M.T., 2002. *Porites* corals as recorders of mining and environmental impacts: Misima Island, Papua New Guinea. Geochem. Cosmochim. Acta 66 (1), 45−62. https://doi.org/10.1016/S0016-7037(01)00715-3.

Fan, Q., Sun, Q., Sui, J., Li, N., 2008. Trace element and isotopic geochemistry of volcanic rocks and its techtonic implications in Weizhou Island and Xieyang Island, Northern Bay. Acta Petrol. Sin. 24 (6), 1323−1332.

Ge, T., Tian, Y., Wang, Q., 2008. Distribution of rare earth elements during estuarine mixing in Beihai Peninsula, Guanxi. J. Chin. Rare Earth Soc. 26 (6), 753−759. https://doi.org/10.3321/j.issn:1000-4343.2008.06.017.

Greaves, M.J., Elderfield, H., Sholkovitz, E.R., 1999. Aeolian sources of rare earth elements to the Western Pacific Ocean. Mar. Chem. 68 (1−2), 31−38. https://doi.org/10.1016/S0304-4203(99)00063-8.

Greaves, M.J., Elderfield, H., Sholkovitz, E.R., 2001. Corrigendum to AAeolian sources of rare earth elements to the Western Pacific Ocean. Mar. Chem. 74 (4), 319. https://doi.org/10.1016/S0304-4203(01)00018-4.

Haley, B.A., Klinkhammer, G.P., McManus, J., 2004. Rare earth elements in pore water of marine sediments. Geochem. Cosmochim. Acta 68 (6), 1265−1279. https://doi.org/10.1016/j.gca.2003.09.012.

Hara, Y., Obata, H., Doi, T., Hongo, Y., Gamo, T., Takeda, S., Tsuda, A., 2009. Rare earth elements in seawater during an iron-induced phytoplankton bloom of the western subarctic Pacific (SEEDS-II). Deep Sea Res. Part II 56 (26), 2839−2851. https://doi.org/10.1016/j.dsr2.2009.06.009.

Hatje, V., Bruland, K.W., Flegal, A.R., 2016. Increases in anthropogenic gadolinium anomalies and rare earth element concentrations in San Francisco Bay over a 20 year record. Environ. Sci. Technol. 50 (8), 4159−4168. https://doi.org/10.1021/acs.est.5b04322.

Jiang, et al., 2017. Coral trace metal of natural and anthropogenic influences in the northern South China Sea. Sci. Total Environ. 607, 195−203. https://doi.org/10.1016/j.scitotenv.2017.06.105.

Jiang, et al., 2018. Annual REE signal of East Asian winter monsoon in surface seawater in the northern South China Sea: evidence from a century-long Porites coral record. Paleoceanography and Paleoclimatology 33, 168−178. https://doi.org/10.1002/2017PA003267.

Kelly, A.E., Reuer, M.K., Goodkin, N.F., Boyle, E.A., 2009. Lead concentrations and isotopes in corals and water near Bermuda, 1780-2000. Earth Planet. Sci. Lett. 283 (1−4), 93−100. https://doi.org/10.1016/j.epsl.2009.03.045.

Koppi, A.J., Edis, R., Field, D.J., Geering, H.R., Klessa, D.A., Cockayne, D.J.H., 1996. Rare earth element trends and cerium−uranium−manganese associations in weathered rock from Koongarra, northern territory, Australia. Geochem. Cosmochim. Acta 60 (10), 1695−1707. https://doi.org/10.1016/0016-7037(96)00047-6.

Kulaksız, S., Bau, M., 2013. Anthropogenic dissolved and colloid/nanoparticle-bound samarium, lanthanum and gadolinium in the Rhine River and the impending destruction of the natural rare earth element distribution in rivers. Earth Planet. Sci. Lett. 362, 43−50. https://doi.org/10.1016/j.epsl.2012.11.033.

Lawrence, M.G., Greig, A., Collerson, K.D., Kamber, B.S., 2006. Rare earth element and yttrium variability in South East Queensland waterways. Aquat. Geochem. 12 (1), 39−72. https://doi.org/10.1007/s10498-005-4471-8.

Lewis, S.E., Shields, G.A., Kamber, B.S., Lough, J.M., 2007. A multi-trace element coral record of land-use changes in the Burdekin River catchment, NE Australia. Palaeogeogr. Palaeoclimatol. Palaeoecol. 246 (2−4), 471−487. https://doi.org/10.1016/j.palaeo.2006.10.021.

Liu, C.Q., Masuda, A., Okada, A., Yabuki, S., Zhang, J., Fan, Z.L., 1993. A geochemical study of loess and desert sand in northern China - implications for continental-crust weathering and composition. Chem. Geol. 106 (3−4), 359−374. https://doi.org/10.1016/0009-2541(93)90037-J.

Liu, Y., et al., 2011. Interannual variation of rare earth element abundances in corals from northern coast of the South China Sea and its relation with sea-level change and human activities. Mar. Environ. Res. 71 (1), 62−69. https://doi.org/10.1016/j.marenvres.2010.10.003.

Liu, Y., et al., 2015. Obliquity pacing of the western pacific intertropical convergence zone over the past 282,000 years. Nat. Commun. 6 https://doi.org/10.1038/ncomms10018.

Liu, Z.F., et al., 2016. Source-to-sink transport processes of fluvial sediments in the South China Sea. Earth Sci. Rev. 153, 238−273. https://doi.org/10.1016/j.earscirev.2015.08.005.

Lo, Li, et al., 2014. Determination of element/Ca ratios in foraminiferal and coral using cold- and hot-plasma techniques on inductively coupled plasma sector field mass spectrometry. J. Asian Earth Sci. 81, 115−122. https://doi.org/10.1016/j.jseaes.2013.11.016.

Ma, J.L., Wei, G.J., Xu, Y.G., Long, W.G., Sun, W.D., 2007. Mobilization and re-distribution of Major and trace elements during extreme weathering of basalt in Hainan Island, South China. Geochem. Cosmochim. Acta 71 (13), 3223−3237. https://doi.org/10.1016/j.gca.2007.03.035.

Ma, W., Chai, F., Xiu, P., Xue, H., Tian, J., 2014. Simulation of export production and biological pump structure in the South China Sea. Geo Mar. Lett. https://doi.org/10.1007/s00367-014-0384-0.

McCulloch, M., Fallon, S., Wyndham, T., Hendy, E., Lough, J., Barnes, D., 2003. Coral record of increased sediment flux to the inner Great Barrier Reef since European settlement. Nature 421 (6924), 727−730. https://doi.org/10.1038/nature01361.

McLennan, S.M., 1989. Rare earth elements in sedimentary rocks: influence of provenance and sedimentary processes. Geochemistry and Mineralogy of Rare Earth Elements. In: Lipin, B.R., McKay, G.A. (Eds.), Rev. Mineral., vol. 21, pp. 169−200.

Moffett, J.W., 1994. A radiotracer study of cerium and manganese uptake onto suspended particles in Chesapeake Bay. Geochem. Cosmochim. Acta 58 (2), 695−703. https://doi.org/10.1016/0016-7037(94)90499-5.

Nozaki, Y., Dobashi, F., Kato, Y., Yamamoto, Y., 1998. Distribution of Ra isotopes and the ^{210}Pb and ^{210}Po balance in surface seawaters of the mid Northern Hemisphere. Deep-Sea Res. I 45 (8), 1263−1284. https://doi.org/10.1016/S0967-0637(98)00016-8.

Nozaki, Y., Lerche, D., Alibo, D.S., Tsutsumi, M., 2000. Dissolved indium and rare earth elements in three Japanese rivers and Tokyo Bay: evidence for anthropogenic Gd and in. Geochem. Cosmochim. Acta 64 (23), 3975−3982. https://doi.org/10.1016/S0016-7037(00)00472-5.

Nguyen, A., Zhao, J., Feng, Y., Hu, W., Yu, K., Gasparon, M., Pham, T., Clark, T., 2013. Impact of recent coastal development and human activities on Nha Trang Bay, Vietnam: evidence from a *Porites lutea* geochemical record. Coral Reefs 32 (1), 181−193. https://doi.org/10.1007/s00338-012-0962-4.

Paytan, A., Kastner, M., 1996. Benthic Ba fluxes in the central Equatorial Pacific, implications for the oceanic Ba cycle. Earth Planet. Sci. Lett. 142 (3−4), 439−450. https://doi.org/10.1016/0012- 821x(96)00120-3.

Saha, N., Webb, G.E., Zhao, J.-X., 2016. Coral skeletal geochemistry as a monitor of inshore water quality. Sci. Total Environ. 566, 652−684. https://doi.org/10.1016/j.scitotenv.2016.05.066.

Saha, et al., 2019. Coral-based high-resolution rare earth element proxy for terrestrial sediment discharge affecting coastal seawater quality, Great Barrier Reef. Geochem. Cosmochim. Acta 254, 173−191. https://doi.org/10.1016/j.gca.2019.04.004.

Schlitzer, R., 2015. Ocean Data View 4. http://odv.awi.de/.

Shen, G.T., Boyle, E.A., Lea, D.W., 1987. Cadmium in corals as a tracer of historical upwelling and industrial fallout. Nature 328 (6133), 794−796. https://doi.org/10.1038/328794a0.

Shen, C.-C., Lee, T., Chen, C.-Y., Wang, C.-H., Dai, C.-F., Li, L.-A., 1996. The calibration of D[Sr/Ca] versus sea surface temperature relationship for *Poirtes* corals. Geochem. Cosmochim. Acta 60 (20), 3849−3858. https://doi.org/10.1016/0016-7037(96)00205-0.

Shen, C.-C., Lu, C., Lo, L., Qu, D., Wei, K.-Y., Gagan, M.K., 2006. Determination of Mg/Ca and Sr/Ca ratios in microgram-quantity coral and foraminiferal samples with permil-level precision by cold plasma inductively plasma sector field mass spectrometry. Eos Trans. AGU 87 (52). Fall Meet. Suppl. Abstract V21A-0544.

Shen, C.-C., et al., 2011. Measurements of natural carbonate rare earth elements in femtogram quantities by inductive coupled plasma sector field mass spectrometry. Anal. Chem. 83 (17), 6842−6848. https://doi.org/10.1021/ac201736w.

Sholkovitz, E.R., Landing, W.M., Lewis, B.L., 1994. Ocean particle chemistry - the fractionation of rare-earth elements between suspended particles and seawater. Geochem. Cosmochim. Acta 58 (6), 1567−1579. https://doi.org/10.1016/0016-7037(94)90559-2.

Sholkovitz, E.R., Shen, G.T., 1995. The incorporation of rare-earth elements in modern coral. Geochem. Cosmochim. Acta 59 (13), 2749−2756. https://doi.org/10.1016/0016-7037(95)00170-5.

Sholkovitz, E.R., Elderfield, H., Szymczak, R., Casey, K., 1999. Island weathering: river sources of rare earth elements to the Western Pacific Ocean. Mar. Chem. 68 (1−2), 39−57. https://doi.org/10.1016/S0304-4203(99)00064-X.

Spivack, A.J., Wasserburg, G.J., 1988. Neodymium isotopic composition of the Mediterranean outflow and the eastern North Atlantic. Geochem. Cosmochim. Acta 52 (12), 2767−2773. https://doi.org/10.1016/0016-7037(88)90144-5.

Sun, R.Y., Hintelmann, H., Liu, Y., Li, X.H., Dimock, B., 2016. Two centuries of coral skeletons from the northern south China sea record mercury emissions from modern Chinese wars. Environ. Sci. Technol. 50 (11), 5481−5488. https://doi.org/10.1021/acs.est.5b05965.

Sun, Y., Sun, M., Lee, T., Nie, B., 2005. Influence of seawater Sr content on coral Sr/Ca and Sr thermometry. Coral Reefs 24 (1), 23−29. https://doi.org/10.1007/s00338-004-0467-x.

Tang, D.L., Kawamura, H., Lee, M.A., Van Dien, T., 2003. Seasonal and spatial distribution of chlorophyll-a concentrations and water conditions in the Gulf of Tonkin, South China Sea. Remote Sens. Environ. 85 (4), 475−483. https://doi.org/10.1016/S0034-4257(03)00049-X.

Wang, P.X., Bradshaw, M., Ganzei, S.S., Tsukawaki, S., Hanssan, K.B., Hantoro, W.S., Poobrasert, S., Burne, R., Zhao, Q.H., Kagami, H., 1997. West Pacific marginal seas during last glacial maximum: amplification of environmental signals and its impact on monsoon climate. In: Proceedings of the 30th International Geological Congress, vol. 13, pp. 65−85.

Wyndham, T., McCulloch, M., Fallon, S., Alibert, C., 2004. High-resolution coral records of rare earth elements in coastal seawater: biogeochemical cycling and a new environmental proxy. Geochem. Cosmochim. Acta 68 (9), 2067−2080. https://doi.org/10.1016/j.gca.2003.11.004.

Xiong, S.F., Sun, D.H., Ding, Z.L., 2002. Aeolian origin of the red earth in southeast China. J. Quat. Sci. 17 (2), 181−191. https://doi.org/10.1002/jqs.663.

Xu, et al., 2018. Oil spill recorded by skeletal δ^{13}C of Porites corals in Weizhou island, Beibu gulf, northern south China sea. Estuarine. Coastal and Shelf Science 207, 338−344. https://doi.org/10.1016/j.ecss.2018.04.031.

Yu, K.F., Jiang, M.X., Cheng, Z.Q., Chen, T.G., 2004. Latest forty two years' sea surface temperature change of Weizhou Island and its influence on coral reef ecosystem. Chin. J. Appl. Ecol. 15 (3), 506−510.

Zhang, J., Nozaki, Y., 1998. Behavior of rare earth elements in seawater at the ocean margin: a study along the slopes of the Sagami and Nankai troughs near Japan. Geochem. Cosmochim. Acta 62 (8), 1307−1317. https://doi.org/10.1016/S0016-7037(98)00073-8.